BIOCHEMISTRY
including biophysical chemistry & molecular biology

Article

pubs.acs.org/biochemistry

Q-Site Occupancy Defines Heme Heterogeneity in *Escherichia coli* Nitrate Reductase A (NarGHI)

Justin G. Fedor, Richard A. Rothery, Karissa S. Giraldi,[†] and Joel H. Weiner*

Membrane Protein Disease Research Group, Department of Biochemistry, University of Alberta, Edmonton, Alberta T6G 2H7, Canada

Supporting Information

ABSTRACT: The membrane subunit (NarI) of *Escherichia coli* nitrate reductase A (NarGHI) contains two *b*-type hemes, both of which are the highly anisotropic low-spin type. Heme b_D is distal to NarGH and constitutes part of the quinone binding and oxidation site (Q-site) through the axially coordinating histidine-66 residue and one of the heme b_D propionate groups. Bound quinone participates in hydrogen bonds with both the imidazole of His66 and the heme propionate, rendering the EPR spectrum of the heme b_D sensitive to Q-site occupancy. As such, we hypothesize that the heterogeneity in the heme b_D EPR signal arises from the differential occupancy of the Q-site. In agreement with this, the heterogeneity is dependent upon growth conditions but is still apparent when NarGHI is expressed in a strain lacking cardiolipin. Furthermore, this heterogeneity is sensitive to Q-site variants, NarI-G65A and NarI-K86A, and is collapsible by the binding of inhibitors. We found that the two main g_z components of heme b_D exhibit differences in reduction potential and pH dependence, which we posit is due to differential Q-site occupancy. Specifically, in a quinone-bound state, heme b_D exhibits an $E_{m,8}$ of −35 mV and a pH dependence of −40 mV pH^{-1}. In the quinone-free state, however, heme b_D titrates with an $E_{m,8}$ of +25 mV and a pH dependence of −59 mV pH^{-1}. We hypothesize that quinone binding modulates the electrochemical properties of heme b_D as well as its EPR properties.

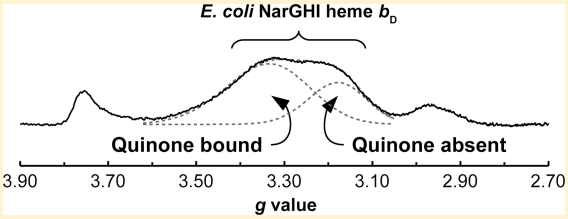

Nitrate reductase A (NarGHI) from *Escherichia coli* is a membrane-bound quinol:nitrate oxidoreductase that is expressed under anaerobic conditions in the presence of nitrate.[1] It functions as a terminal reductase, coupling quinol oxidation to nitrate reduction, and contributes to the generation of a proton electrochemical potential across the cytoplasmic membrane.[2] NarGHI comprises a catalytic subunit (NarG, 140 kDa), an electron-transfer subunit (NarH, 58 kDa), and a membrane anchor subunit (NarI, 26 kDa). NarG contains a molybdo-bis(pyranopterin guanine dinucleotide) (Mo-bisPGD) cofactor that is the site of nitrate reduction as well as a single tetranuclear iron−sulfur ([4Fe−4S]) cluster known as FS0. NarH contains three [4Fe−4S] clusters (FS1−FS3) and one trinuclear iron−sulfur cluster ([3Fe−4S], FS4). NarI anchors the NarGH subunits to the inside of the cytoplasmic membrane and contains two hemes *b* that are proximal (b_P) and distal (b_D) to the NarGH subunits, respectively. Overall, these subunits provide a molecular scaffold for an electron-transfer relay connecting the site of quinol oxidation adjacent to heme b_D in NarI (the Q-site) with the Mo-bisPGD of NarG.[3,4] NarGHI is a robust enzyme that is readily expressed to levels approaching spectroscopic purity in *E. coli* cytoplasmic membrane preparations, rendering it an excellent system for studying redox cofactor spectroscopy and electrochemistry.[5−10] Although the overall architecture of the enzyme has been defined by X-ray crystallography, the factors controlling reactivity at the Mo-bisPGD and Q-sites are far from being fully understood.

The redox properties and reduction potentials of the NarGHI cofactors have been extensively studied using a combination of spectroscopic[7] and potentiometric methods.[8,10] In general, electrons flow in the overall thermodynamically downhill direction from menaquinol (MQ) or ubiquinol (UQ) through the two hemes of NarI, the four [Fe−S] clusters of NarH, and then through the single [4Fe−4S] cluster of NarG to the Mo-bisPGD cofactor, where nitrate is reduced to nitrite. One of the hemes of NarI, heme b_D, is in close juxtaposition to the Q-site identified by protein crystallography.[11] Elements of the heme, including one of this propionate groups and one of its iron-coordinating His residues (His66), directly participate in hydrogen-bonding interactions with the bound Q-site inhibitor pentachlorophenol (PCP) observed in one of the available structures (PBD 1Y4Z) (Figure 1). This results in the EPR spectrum and reduction potential of heme b_D being exquisitely sensitive to the presence of quinol analogue inhibitors in the Q-site. NarGHI is able to oxidize both major quinol species found in the *E. coli* cytoplasmic membrane:[12] ubiquinol dominates under oxidizing and oxic conditions, whereas menaquinol dominates under reducing and anoxic conditions. This raises the question of how the composition of the quinol pool impacts the spectroscopic and functional properties of heme b_D.

Received: January 28, 2014
Revised: March 3, 2014
Published: March 4, 2014

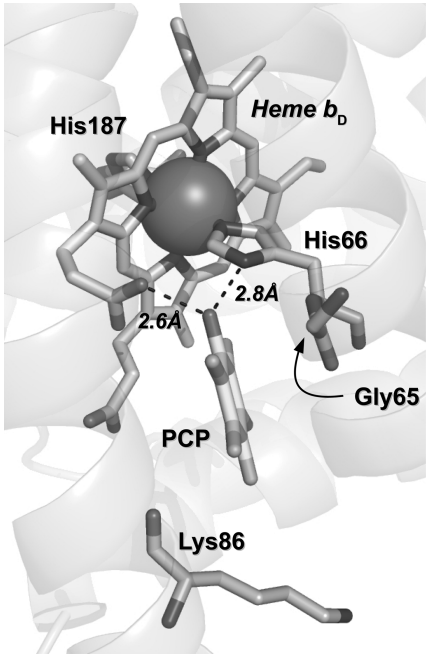

Figure 1. Q-site of NarI with pentachlorophenol bound. Coordinating heme b_D are His187 and His66, which also hydrogen bonds with bound PCP and semiquinones.[11] Image generated using PyMol and PDB 1Y4Z.[11,52]

The two hemes of NarI exhibit highly anisoptropic low-spin (HALS) spectra with reported g_z values of approximately 3.76 and 3.36 for heme b_P and b_D, respectively.[10] Heterogeneity of heme b_D has been reported in a mutant unable to synthesize Mo-bisPGD,[13] resulting in the appearance of two components with g_z values of approximately 3.35 and 3.21. Arias-Cartin et al.[14] also reported that heme b_D can exist in two forms, one with a g_z of approximately 3.20 and the other with a g_z of approximately 3.35. Extraction of hydrophobic components using dodecylmaltoside (DDM) resulted in diminution of the g = 3.20 component and retention of the g = 3.35 component. These effects were interpreted to arise from the DDM-induced leaching of a tightly bound cardiolipin molecule from the membrane intrinsic region of NarGHI. In this article, we test the alternative hypothesis that quinone composition and binding are the determinants of heme b_D heterogeneity. We present evidence that the two components arise from specific quinone-bound and quinone-free populations of NarGHI within the *E. coli* inner membrane.

MATERIALS AND METHODS

Bacterial Strains, Plasmids, and Membrane Vesicle Preparation. Wild-type NarGHI was overexpressed in *E. coli* strains LCB79 (*araD*139 Δ(*lac*I-POZYA-*argF*) *rpsL*, *thi*, Φ79(*nar-lac*)),[15] the cardiolipin-deficient strain S330 (W3110 *ksgB1 lpp-2 pgsA30*::*kan*),[16] the napthoquinone (menaquinone, demethylmenaquinone)-deficient strain JCB4111 (JCB4011 Δ*menBC*),[17] the ubiquinone-deficient JCB4211 (JCB4011 Δ*ubiCA*),[17] and the cytochrome-deficient strains JW0723 (W3110 Δ*cydB*) and JW0421 (W3110 Δ*cyoB*).[18] The expression vector used was pVA700 (*tacP*, *rrnB*, *lacI*^{q}, amp^r, *narGHJI*).[19] Growth of LCB79, JCB4111, and JCB4211 was supplemented with 100 mg L^{-1} of streptomycin; for S330, JW0723, and JW0421, 50 mg L^{-1} of kanamycin was used, and for all strains bearing the pVA700 expression vector, 100 mg L^{-1} of ampicillin was added to the cultures. Cell growth in 2 L batches of Terrific Broth[20] was performed as previously described.[10] Fermenter growths were conducted in 5 or 10 L batches in either fermenter broth or glycerol-peptone-fumarate (GPF) (anaerobic growth)[21] at pH 7.0 using 2 M NaOH and 1 M HCl for pH adjustments.[11] The GPF was supplemented with 4 mM KNO_3, 0.003% (w/v) leucine, and 0.003% (w/v) threonine. Fermenter broth contains 12 g L^{-1} of tryptone, 24 g L^{-1} of yeast extract, 5 g L^{-1} of NaCl, 0.56% (v/v) glycerol, and 200 mg L^{-1} of thiamine hydrochloride; note that overnight precultures of fermenter broth use 0.4% (v/v) glycerol. Inoculation was accomplished with 10% (v/v) overnight cultures grown at 37 °C, 225 rpm in flasks containing Terrific or fermenter Broth.[11] When the OD_{600} reached 0.5 (Anaerobic, GPF culture) or 2.0 (Semianaerobic, FB cultures), 1 mM isopropyl-1-thio-β-D-galactopyranoside (IPTG) was added to induce NarGHI expression from pVA700.[11] Stir speed, postinduction incubation temperature, and aeration rates are detailed in the legend of Figure 2. The buffer system used for vesicle preparations contained 5 mM EDTA as well as either 100 mM 2-(*N*-morpholino)ethanesulfonic acid (MES), 100 mM 3-(*N*-morpholino)propanesulfonic acid (MOPS), 100 mM Tricine, or 100 mM *N*-cyclohexyl-2-aminoethanesulfonic acid (CHES) for pH 6.0, 7.0, 8.0, and 9.0, respectively. The processing of the cells has been previously outlined[10] and included the addition of 0.2 mM phenylmethylsulfonyl fluoride prior to emulsiflexing three to five times. Throughout the processing procedure, 100 mM MOPS and 5 mM EDTA buffer (pH 7.0) was used until the final two resuspensions, where the appropriate buffer for pH poising was used. All samples were resuspended to ∼30 mg mL^{-1}, flash frozen as aliquots in liquid nitrogen, and stored at −80 °C.

Redox Potentiometry and EPR Spectroscopy. Redox titrations were conducted under argon at 25 °C in the pH-specific buffers mentioned earlier, as previously described.[10,22,23] Redox titrations require the inclusion of 25 μM each of the following redox mediators (dyes) prepared as 50 mM aqueous stock solutions: quinhydrone (+287 mV), 2,6-dichlorophenolindolphenol (+217 mV), 1,2-naphthoquinone (+125 mV), toluylene blue (+115 mV), phenazine methosulfate (+80 mV), thionine (+60 mV), methylene blue (−11 mV), resorufin (−50 mV), indigo trisulfonate (−80 mV), indigo carmine (−125 mV), anthraquinone-2-sulfonic acid (−225 mV), phenosafranine (−255 mV), and neutral red (−329 mV).[23] All samples were taken in 3 mm i.d. quartz EPR tubes, rapidly frozen using liquid-nitrogen-chilled ethanol, and stored at −70 °C prior to use. EPR spectra were acquired as previously described[10] using a Bruker Elexsys E500 series X-band EPR spectrometer (9.38 GHz) with an ESR-900 flowing helium cryostat, a temperature of 10−12 K, and a 10 G_{pp} modulation amplitude at 100 kHz. All potentials are relative to the standard hydrogen electrode, and, unless otherwise mentioned, the depicted spectra are poised at approximately +280 mV. See figure legends for microwave power (MWP) levels used. Baseline correction for Gaussian deconvolution analysis was conducted by using a derivative Lorentzian line shape, which gave superior fits to third−fifth-order polynomial baselines as well as derivative Gaussian line shapes.[24] The area-normalized equation used for derivative Lorentzian baseline correction is

$$\frac{dY}{dx} = -S\left(\frac{2L^2(x - x_o)}{(L^2 + (x - x_o)^2)^2}\right) + Dx + A$$

dx.doi.org/10.1021/bi500121x | *Biochemistry* 2014, 53, 1733−1741

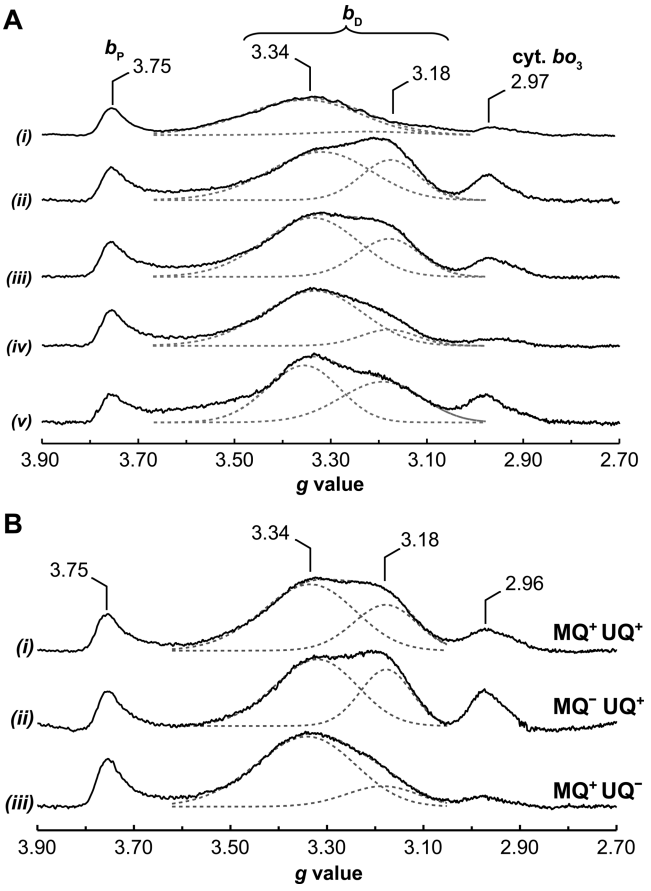

Figure 2. Effects of growth conditions and quinones on heme b_D EPR line shape are apparent in redox-poised oxidized heme spectra of NarGHI hemes b_P (g = 3.75) and b_D (g = 3.0–3.4). The *g*-value labels indicate the average maximum *g* value over the range of applied potentials. (A) Effects of growth conditions (oxygenation) on heme b_D heterogeneity. Spectrum (i) is of pH 7 membranes obtained from 2 L batches of cells grown overnight at 30 °C at very low agitation in 6 L nonbaffled Erlenmeyer flasks. Spectra (ii–iv) depict the effect of aerobic to increasingly more anaerobic growth conditions: (ii) 10 L vessel, 2 L min^{-1} aeration, and 500 rpm impeller stir rate, pH 7 membranes; (iii) 5 L vessel, 500 rpm stirring, <1 L min^{-1} aeration, pH 8 membranes; and (iv) 10 L vessel, 200 rpm stirring, no aeration, pH 8 membranes. Spectrum (v) is of NarGHI expressed in a cardiolipin-deficient strain (S330), flask grown, pH 7 membranes. The sample spectra (i–v) were respectively poised at: +266, +279, +292, +274, and +278 mV. (B) Effects of MQ and UQ on the heme b_D EPR signal: (i) 10 L vessel, 2 L min^{-1} aeration, and 500 rpm impeller stir rate, pH 7 LCB79/pVA700 membranes poised at +279 mV; (ii) NarGHI expressed in a menaquinone-deficient strain (JCB4111/pVA700) grown in a 5 L vessel, 500 rpm stirring, <1 L min^{-1} aeration, pH 8 membranes poised at +280 mV; and (iii) NarGHI expressed in a ubiquinone-deficient strain (JCB4211/pVA700) grown in a 10 L vessel, 200 rpm stirring, no aeration, pH 8 membranes poised at +281 mV. Spectra were collected at 10 K and 4 mW (17 dB) MWP except for (i), which was collected at 10 dB MWP.

where *S* is a scale factor and is equal to half of the peak-to-peak amplitude, *L* is the line width at half-peak height, x_o is the *x* intercept of the derivative, *D* is the linear slope, and *A* is the linear *y* intercept. This satisfactorily simulates the interfering portion of the junk iron signal at *g* = 4.3 that causes the extreme extent of the baseline at low field ($g < 3.75$).[25] Baseline correction and Gaussian deconvolution was conducted by nonlinear least-squares fitting via the Levenberg–Marquadt method using Matlab (version R2013b, The MathWorks Inc., Natick, MA).

Enzyme Assays. The Lowry procedure for protein concentration determination was modified to include 1% (w/v) SDS for solubilization of membrane proteins.[26,27] Quinol:nitrate oxidoreductase assays were conducted using the quinol analogue plumbagin (PB).[28] Stock solutions were prepared with 100% anhydrous ethanol at concentrations of 20 mM PB and then stored at −20 °C. Zinc powder was used as a reductant, where ∼70 mg of Zn^0 and 1.7 mL of PB solution were added to a 2 mL HPLC vial followed by addition of 60 μL 5 M HCl(aq). The vials were then sealed with a rubber septum and shielded from light with aluminum foil. The assay buffer consisted of 100 mM MOPS, 5 mM EDTA, 4 mM KNO_3, and 30 mM glucose at pH 7.0 and was degassed on a vacuum line for ≥1 h prior to use. Individual assays were conducted in 1.0 cm two-sided acryl cuvettes fitted with two-holed tight-fitting Teflon stoppers and a stir bar. To ensure anaerobic conditions, 5 μL of ≥200 U mg^{-1} low catalase activity (≤0.1 U mg^{-1}) glucose oxidase solution (Sigma-Aldrich G0543) was added to the cuvette; it was topped up with reaction buffer, and then the stopper was inserted such that no air bubbles remained in the cuvette (this volume was determined to be 2.98 ± 0.04 mL). Typically, 10–20 μL of a 1:1 to 1:5 dilution of protein sample (∼30 mg mL^{-1}) was added via Hamilton syringe, and then the blank measurement was taken. The reaction was initiated by addition via Hamilton syringe of 50 μL of plumbagin to give a final concentration of 0.33 mM. The Q-site independent (nonspecific) reductant benzyl viologen (BV) was used to monitor nitrate reduction activity independent of quinol oxidation activity. The assay was conducted similar to the PB:NO_3 assay; however, an aqueous stock solution of 6.1 mM BV was prepared, and a 20 mM solution (1 M Tris, pH 9.0) of sodium dithionite was used to reduce the BV. To a stoppered cuvette filled with buffer, vesicles, and 50–100 μL of dithionite was added 100 μL BV. Assays were conducted on an HP8453 diode array spectrophotometer equipped with a HP 89090A Peltier temperature controller/cuvette stirrer set to a stir rate of 200 rpm, 25 °C. Baseline correction of A_{419} minus the average ($A_{695} - A_{700}$) was used for rate calculation of the PB:NO_3 assay. The relevant chemical parameters for plumbagin are λ_{max} = 419 nm and ε_{419} = 3.95 mM^{-1} cm^{-1}, and for BV, λ_{max} = 570 nm and ε_{570} = 7.8 mM^{-1} cm^{-1}.[28]

RESULTS

Growth Conditions Influence Heme b_D Heterogeneity. Figure 2A(i) shows a representative EPR spectrum of the NarGHI hemes in redox-poised oxidized membranes derived from cells grown on rich media with essentially no aeration.[10] This spectrum exhibits a sharp peak at approximately *g* = 3.75 arising from heme b_P and a broad peak centered at approximately 3.34 that arises from heme b_D. A minor peak at *g* = 2.97 can be assigned to the cytochrome bo_3 ubiquinol:oxygen oxidoreductase (see Supporting Information Figure 1). (For the sake of clarity, *g* values observed in this work will be quoted throughout. Minor differences in *g* values between contributions likely arise from subtle differences in preparations and instrument calibrations.) We investigated the effect of growth-culture aeration by recording heme EPR spectra of NarGHI-containing membranes from cells grown at high (Figure 2A(ii)), intermediate (Figure 2A(iii)), and low (Figure 2A(iv)) levels of culture aeration. These three spectra exhibit heterogeneity comprising two peaks centered at *g* = 3.34

dx.doi.org/10.1021/bi500121x | *Biochemistry* 2014, 53, 1733–1741

and 3.18, with diminishing intensity of the latter feature with decreasing aeration.

It has been suggested that heme b_D heterogeneity is due to a mixture of enzyme with and without a tightly bound cardiolipin.[14] In this context, the heme b_D EPR signal heterogeneity has been interpreted such that the g = 3.18 signal is due to cardiolipin-bound enzyme, and the g = 3.34 signal is due to cardiolipin-free enzyme.[14] To test if cardiolipin does indeed contribute to the heterogeneity, nitrate reductase was expressed semiaerobically in an *E. coli* strain deficient in its biosynthesis as well as for phosphatidylglycerol (*E. coli* S330).[16] As shown the Figure 2A(v), both heme b_D components are still observed in membranes from the cardiolipin-deficient strain. It is therefore unlikely that cardiolipin plays a role in heme b_D heterogeneity in NarGHI.

Influence of Q-Site Structure and Occupancy on Heme b_D EPR Spectra. *E. coli* synthesizes two major types of lipophilic quinones that shuttle electrons from dehydrogenases to reductases within the cytoplasmic membrane. These comprise UQ-8 and MQ-8 and predominate under oxidizing and reducing conditions, respectively.[12,29−31] NarGHI is able to bind and oxidize both major quinol species at its Q-site.[32,33] Given that the heme b_D heterogeneity appears to decrease with decreasing aeration during cell growth and is not eliminated in the absence of cardiolipin we speculated that it may be related to the composition of quinones within the *E. coli* cytoplasmic membrane. Alternative binding modes for the two quinones, which have already been shown to bind to the same Q-site in NarI,[11,34] may account for the two different conformations seen in the EPR spectra of heme b_D.

To test whether heme b_D heterogeneity reflects the differential binding of MQ and UQ, NarGHI was expressed in a strain incapable of producing napthoquinones MQ/DMQ (MQ^-UQ^+), JCB4111 (Δ*menBC*), and a strain incapable of producing UQ (MQ^+UQ^-), JCB4211 (Δ*ubiCA*). *E. coli* JCB4211 (Δ*ubiCA*) can grow only under semiaerobic/anaerobic conditions, and *E. coli* JCB4111 (Δ*menBC*) is unable to grow under anaerobic conditions. The heterogeneity observed in the EPR spectra of heme b_D in Figure 2B is similar to that in Figure 2A; however, in the MQ^+UQ^- strain, the heterogeneity is greatly reduced, with a much lower contribution from the g = 3.18 component. There is no significant effect on signal position of either component, and the difference in heterogeneity can be explained by the differing growth conditions necessary for cultivating membranes from the two strains. The most aerobically grown cultures (MQ^-UQ^+) exhibit the greatest heterogeneity, whereas the most anaerobically grown cultures (MQ^+UQ^-) exhibit the least heterogeneity. The MQ^+UQ^+ culture, being grown less aerobic than MQ^-UQ^+, exhibited intermediate heterogeneity. In general, there is a correlation between a lack of UQ/anaerobic growth conditions and a decreased intensity of the g = 3.18 component.

Quinone Site Variants and Their Effects on Heme b_D. To probe the potential involvement of quinone binding in determining heme b_D heterogeneity further, we investigated several Q-site variants of two conserved residues, Lys86 and Gly65, and the effect of the Q-site inhibitor HOQNO on their heme b_D EPR spectra.[11,35] HOQNO is a menasemiquinone analogue and Q-site inhibitor, which, when added to membranes containing wild-type NarGHI, elicits a collapse of the g = 3.18 and 3.33 components into a single HOQNO-bound form with a peak at g = 3.52 (Figure 3A). NarI-Lys86 is

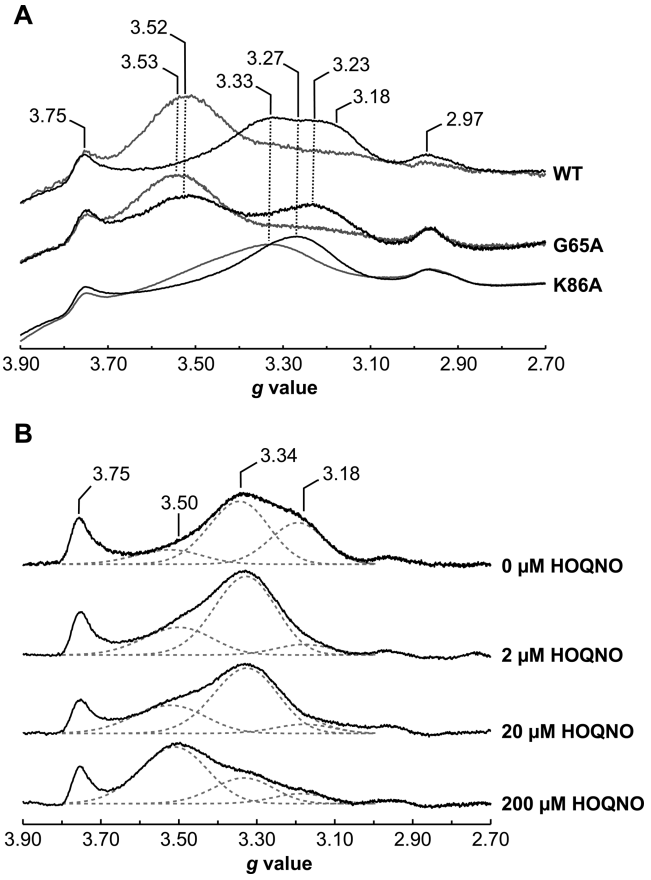

Figure 3. (A) HOQNO binding to Q-site variants K86A and G65A. Black lines represent spectra of oxidized membranes, and gray lines represent spectra of DCPIP-oxidized membranes treated with 0.5 mM HOQNO. (B) HOQNO titration of the heme b_D EPR signal. The spectra obtained are pH 8 membranes redox-poised to about +280 mV. All of the membranes were prepared from flask-grown cultures under standard growth conditions (see Materials and Methods) and contain an approximate concentration of 60−70 μM of NarGHI. Spectra were collected at 10 K and 4 mW (17 dB) MWP.

a highly conserved residue, and it has previously been shown that mutation of this residue to an alanine significantly diminishes quinol:nitrate oxidoreductase activity and semimenaquinone stability.[11,36] Furthermore, the redox-poised heme b_D EPR spectrum manifests as a single peak centered at g = 3.27−3.28 (Figure 3A).[36] Addition of HOQNO to membranes containing the K86A variant elicits a minor shift of the heme b_D peak from g = 3.27 to 3.33. The K86A variant does not support growth and has diminished quinol:nitrate oxidoreductase activity (Table 1). NarI-Gly65 is another highly conserved residue lining the Q-site of NarGHI,[11] and we generated a G65A variant. This retains two heme b_D components in its EPR spectrum at g = 3.23 and 3.52, which collapse into a single g = 3.53 peak of greater intensity upon treatment with HOQNO (Figure 3A). It is notable that the G65A is able to support growth and retains significant quinol:nitrate oxidoreductase activity (Table 1).

Effect of HOQNO on the Heme b_D Spectrum Is Concentration-Dependent. What is unclear from the HOQNO-binding experiments outlined earlier is whether both components are equally sensitive to inhibitor binding. Figure 3B shows the effects of titrating HOQNO into oxidized wild-type NarGHI membranes. First, the g = 3.18 component

dx.doi.org/10.1021/bi500121x | *Biochemistry* 2014, 53, 1733−1741

Table 1. NarI Variant Plumbagin:Nitrate Oxidoreductase Activities[a]

NarI variant	μmol benzyl viologen (mg^{-1} min^{-1})	μmol plumbagin (mg^{-1} min^{-1})	PB/BV	growth on nitrate
wild-type	63.6	3.37	53 (100%)	+++
G65A	21.5	0.79	38 (69%)	++
K86A	30.3	0.25	8 (16%)	−

[a]The activities of the plumbagin and benzyl viologen oxidation and nitrate reduction for the NarI variants tested are represented as mean values of at least triplicate experiments with standard errors less than 10%. Anaerobic growth on glycerol:nitrate is depicted in Supporting Information Figure 2.

collapses concomitant with a rise in the g = 3.50 component. In the presence of higher concentrations of HOQNO, the signal at g = 3.34 begins to shift to g = 3.50. This, therefore, indicates that the g = 3.18 conformation of NarI has a greater ability to bind HOQNO compared to the g = 3.34 conformation.

Redox Potentiometry of the g = 3.34 and 3.18 Components of NarI Heme b_D. The biophysical characteristics of hemes are known to be influenced by the surrounding protein environment. In the case of heme b_D, there appears to be two distinct environments that are resolvable by EPR spectroscopy. Given the link between quinone pool composition/growth conditions and the intensity of the g = 3.18 component (Figure 2B), we speculated that investigating the pH dependence of the reduction potentials of the two components may shed light on their origins. The g = 3.18 and 3.34 components titrate with reduction potentials of +25 and −35 mV at pH 8.0, respectively (Figure 4A). The integrated intensity of the spectrum encompassing both peaks titrates with reduction potentials of +25 (25%) and −35 mV (75%). When titrations are carried out at a range of pH values between 6.0 and 9.0, the g = 3.18 and 3.34 components exhibit dependencies of −59 and −40 mV pH^{-1}, respectively (Figure 4B). These observations suggest that the form of NarI giving rise to the g = 3.18 peak has an ionizable group in the vicinity of heme b_D that is tightly coupled to the pH of the aqueous milieu (reduction results in the uptake of one proton per electron), whereas the g = 3.34 form is more weakly coupled.

Examination of redox-poised EPR spectra at either end of the pH range in Figure 4C reveals that the g = 3.18 component is favored under acidic conditions, collapsing to the g = 3.34 conformation at higher pH. The single integration of the entire heme b_D EPR signal shows interconversion of the two forms with no significant difference, with the pH 6 signal having an area of 181 and the pH 9 signal, an area of 195. Heme b_P, however, decreases in intensity upon alkalinization: 29 at pH 6 to 19 at pH 9. This is concomitant with an increase in the g = 2.94 component under more alkaline conditions.

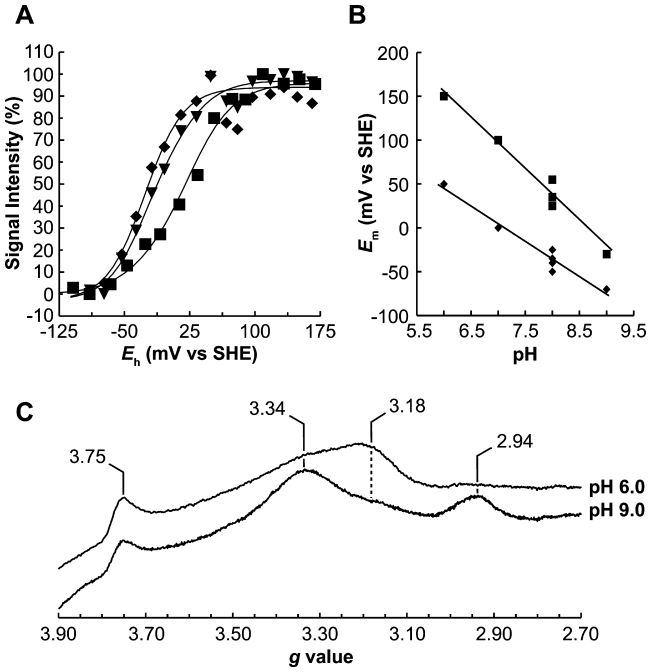

Figure 4. Redox titrations and pH dependence of the components of heme b_D. (A) Redox titration at pH 8 of Δ*cydB*/pVA700 membranes. The g = 3.18 titration (■) was fit with $E_{m,8}$ components of +25 (81%) and −35 mV (15%). The g = 3.34 titration (♦) was fit with a single $E_{m,8}$ of −35 mV. Inverted triangles (▼) represent the data obtained by single integration of the heme b_D signal with baseline correction fit with $E_{m,8}$ components of −35 (75%) and +25 mV (25%) integrated intensity values, and baseline subtraction was done with the software Xepr. The single-component titrations were obtained by doing three-point dropline subtraction at g = 3.81 and 3.05. Fits are modeled with the Nernst equation scaled for average maximum intensity and with an electron stoichiometry of n = 1. The EPR spectra for the titration were obtained at 12 K and 4 mW (17 dB) MWP. (B) Reduction potential pH dependence of heme b_D for the two heme b_D components. The pH dependence of the g = 3.18 component (■) is approximately −59 mV pH^{-1}, whereas the g = 3.34 component (♦) is approximately −40 mV pH^{-1}. (C) Two spectra from a single membrane preparation split into two redox titrations at pH 6.0 and 9.0 poised at +289 and +292 mV, respectively. The increase in pH is concomitant with a decrease in the g = 3.18 component and the g = 3.75 heme b_P signal and an increase in the g = 3.34 and the appearance of a g = 2.94. Using the software Xepr, a fifth-order polynomial baseline correction and integration was conducted on the signals. For g = 3.75, pH 6 = 29 and pH 9 = 19. For g = 3.3 + g = 3.18, pH 6 = 195 and pH 9 = 181. For g = 2.94, pH 6 = 2 and pH 9 = 42. The EPR spectra were acquired at 4 mW (17 dB) MWP 10 K.

■ DISCUSSION

Although the two hemes of NarI have EPR spectra well-resolved from each other, interpretation of the heme b_D EPR properties is complicated by the presence of components appearing at g = 3.34 and 3.18 (Figure 2B). Furthermore, we observed that these two components are dependent upon growth conditions, the composition of the quinone pool, and ambient pH (Figures 2 and 4). Membranes from cells grown at high aeration exhibit more heme b_D heterogeneity, and we established that this can be attributed to multiple subpopulations of NarGHI by recording EPR spectra of membrane samples lacking the two well-characterized *E. coli* quinol:oxygen oxidoreductases that also contain low-spin *b*-type hemes (Supporting Information Figure 1).

Recently, it has been proposed that the two components of heme b_D arise from cardiolipin-bound versus cardiolipin-free states, corresponding to the g = 3.18 and 3.34 peaks, respectively.[14] The cardiolipin headgroup binds to a region within the complex where all three subunits converge and is stabilized by the conserved residues NarG-Tyr9, NarG-Arg6, NarH-Arg218, and NarI-Tyr28. Given that maturation of NarGHI is highly coordinated and involves a redox enzyme maturation protein (NarJ) and sequential insertion of its prosthetic groups,[13,37] it is unlikely that a significant proportion of the mature enzyme would be assembled without the structurally important cardiolipin. It is also unlikely that

dx.doi.org/10.1021/bi500121x | *Biochemistry* 2014, 53, 1733−1741

another anionic phospholipid (phosphatidylglycerol) binds in its place because the S330 strain is defective in phosphatidylglycerol and cardiolipin biosynthesis (*pgsA* null).[16] In either case, the protein structure indicates a fatty acyl chain of cardiolipin is located within 4 Å of His66. It has been proposed that this interacts with and ensures the proper orientation of His66 to ensure effective quinone binding.[14] However, the contact surface is small because the cardiolipin acyl chain lies perpendicular to the His66 imidazole plane and would have a weak van der Waals interaction with it at best. Critically, when NarGHI is expressed in cells deficient in cardiolipin biosynthesis, the EPR spectrum of heme b_D still shows a clear heterogeneity, as seen in Figure 2A(v). As reported by us[11] and Arias-Cartin et al.,[14] the presence of increasing concentrations of detergent clearly decreases the observed heterogeneity of the heme b_D EPR signal. Preparation in Thesit ($C_{12}E_9$)[11] and high concentrations of dodecylmaltoside (DDM) collapse the g = 3.18 signal.[14] However, it is known that detergent binding can have effects on the structure and function of membrane proteins.[38−40] Furthermore, even at high concentrations of DDM (0.15%), a 1:1 molar amount of cardiolipin was found to remain bound to NarGHI, likely the tightly bound cardiolipin molecule implicated in modulating heme b_D conformation.[14] So, interpretation of data obtained for detergent-solubilized NarGHI is complicated at best and may result in physiologically irrelevant results.

As an alternative explanation for the heme b_D heterogeneity, we focused on the role of Q-site occupancy and quinone binding for several reasons. First, it has been previously shown that the EPR spectrum of heme b_D is exquisitely sensitive to the binding of the Q-site inhibitors 2-*n*-heptyl 4-hydroxyquinoline-*N*-oxide (HOQNO), pentachlorophenol (PCP), and stigmatellin.[10,41] Herein, we show that binding of HOQNO collapses the heterogeneity in the heme b_D EPR signal (Figure 3). Second, the heterogeneity is dependent upon growth conditions (Figure 2A), as are the membrane concentrations of menaquinone and ubiquinone.[29,29,42] Third, the extent of heterogeneity is quinone-dependent, with the g = 3.18 component inversely correlated with the availability of UQ and aerobicity of growth condtions (Figure 2B). Finally, we observed that the heterogeneity is sensitive to Q-site variants of Lys86 and Gly65 (Figure 3A). Collectively, these observations clearly indicate a role for Q-site occupancy/structure in heme b_D heterogeneity.

The first possibility is that each component corresponds to the binding of either of the two major types of quinone. This would be logical given that the unique binding characteristics of each inhibitor (HOQNO, PCP, or stigmatellin) elicit specific shifts in position of the heme b_D g_z. However, because the two components are present when either MQ or UQ are present (Figure 2B), the heterogeneity is not due to the binding of one quinone versus the other. Therefore, these two components may be due to alternative binding modes of quinones such as has been proposed for *E. coli* succinate:quinone oxidoreductase (SdhCDAB)[43] or one component corresponds to a Q-site free of quinone and the other to quinone-bound. We have previously observed that binding of the Q-site inhibitor PCP modulates the g_z value of heme b_D as well as the dihedral angle observed in crystal structures,[11] whereas HOQNO has an even larger effect on the spectrum. The correlation between g_z value and bis-His coordination dihedral angle is well-documented, with a larger, more strained g_z value (more anisotropic) resulting from a more perpendicular bis-His interplanar angle, and a more parallel, relaxed orientation giving a lower g_z value (less anisotropic).[44] Because NarGHI preferentially uses MQ, which binds to it with a higher affinity over ubiquinone, and better stabilizes menasemiquinone over ubisemiquinone, one therefore expects the component corresponding to the occupied Q-site conformation to correlate most closely with the presence of MQ.[14,34,45] In the case where MQ is absent (Figure 2B), we observe the most heterogeneity and greatest contribution from the g = 3.18 component. When both MQ and UQ are present, the heterogeneity is reduced, and the g = 3.34 component becomes more prominent. Finally, when *ubiCA* is knocked out, as in JCB4211, the MQ content was found to be actually enhanced by 30% compared to wild-type *E. coli* (MQ^+UQ^+)[46] and consequently the heme heterogeneity is at its lowest extent, with the g = 3.34 component being greatly dominant. Therefore, we propose that the g = 3.34 component is due to an occupied Q-site, especially by MQ, which modulates the His66 coordination geometry of heme b_D via a previously characterized hydrogen bond.[47,48] *Ipso facto*, the g = 3.18 component is due to a unoccupied Q-site conformation of NarI. This is supported by experiments such as that depicted in Figure 3B, wherein increasing concentrations of HOQNO collapse the g = 3.18 component prior to the g = 3.34 component. The collapse of the g = 3.18 component occurs at concentrations less than 2 μM HOQNO (~1:35 mols of HOQNO to NarGHI), whereas the shift in g = 3.34 to 3.50 begins occurring at about a molar ratio of 2:7, with complete conversion accomplished with addition of excess HOQNO (20:7). This is interpreted such that empty Q-sites are occupied by the inhibitor prior to displacement of quinone from occupied sites.

To probe the involvement of the Q-site in defining heme b_D properties further, we looked at the effects of variants of the Q-site residues Gly65 and Lys86. Gly65 is a highly conserved residue in NarI and has a role in defining Q-site functionality.[11] The G65A variant retains substantial quinol:nitrate oxidoreductase activity and is able to support respiratory growth on nitrate, whereas the K86A variant has diminished activity and is unable to support growth (Table 1 and Supporting Information Figure 2). The G65A variant exhibits an EPR spectrum where the g_z values for the two components of the heme b_D signal are more divergent than in the wild-type enzyme (Figure 3A). The g = 3.18 component exhibits a minor shift to g = 3.23; however, the g = 3.34 component shifts to g = 3.52. In the presence of HOQNO, the G65A variant exhibits similar behavior to the wild-type: diminution of the relaxed g = 3.23 component and a shift of the g = 3.52 strained component to g = 3.53 with a concomitant increase in intensity (Figure 3A). The K86A variant has decreased quinol:nitrate oxidoreductase activity and is unable to support anaerobic growth on nitrate (Table 1).[11] HOQNO elicits only a minor effect on the heme b_D spectrum in membrane samples, shifting it from g = 3.27 to g = 3.33 (Figure 3A), with no evidence of two components in the unbound form. These observations suggest that the g = 3.27 feature of the K86A variant EPR spectrum is equivalent to the g = 3.18 feature of the wild-type spectrum and reflects an unoccupied Q-site. Overall, these observations support the hypothesis that heme b_D heterogeneity is linked to Q-site occupancy.

With heme b_D demonstrating two subpopulations, it is likely that these two conformations exhibit different redox properties, as we have previously observed that HOQNO and stigmatellin modulate heme b_D reduction potential by $\Delta E_{m,7}$ +100 and +30

mV, respectively.[10] Redox characterization (Figure 4A) of the two components was carried out by expressing NarGHI in a cytochrome *bd*-deficient strain to eliminate the interfering b_{559} signal (see Supporting Information Figure 1). The free (g = 3.18) component titrates with an $E_{m,8}$ of +25 mV, whereas the $E_{m,8}$ of the occupied component at g = 3.34 is −35 mV. A titration of the first integral heme b_D signal can be fit with a −35 mV component (75%) and a +25 mV component (25%). Figure 4B shows that over the pH range tested the free component consistently titrates at a higher potential than the occupied state. The pH dependence calculated in the present study for the occupied heme b_D conformation of −40 mV pH^{-1} is within agreement of the previously reported value of −36 mV pH^{-1},[23] and a redox-Bohr effect of −59 mV pH^{-1} was calculated for the free conformation. This difference between the two conformations of NarI is likely due to the modulation of His66 and/or heme b_D proprionate pK_a upon quinone binding. Quinone and quinone-analogue binding alters the electrostatic environment of the heme and therefore is expected to modulate heme reduction potential, which would explain the different redox-Bohr effect that we observe for the two conformations as well as the modulation of reduction potential when quinol analogues are present. For example, the reduction potentials of hemes and the protonation state of their proprionates are known to be coupled, with reduced heme having a higher pK_a than oxidized heme. In the case of cytochrome c_{551}, the pK_a shifts from 5.9 in the oxidized state to 7.0 in the reduced state,[49,50] and for surfactant micelles of hemin (diaquo heme *b*) in tetrahydrofuran, the heme proprionates exhibit a pK_a of 6.5 in the ferric form and 7.5 in the ferrous form.[51] We also observe a pH dependence for the heterogeneity: Figure 4C shows that the g = 3.18 form is favored at low pH, whereas a high pH collapses this component to the g = 3.34 conformation. Therefore, the Q-site occupied conformation seems to be favored at high pH, and the free conformation, at low pH. This pH dependence of stabilization of the two conformations may be tied to the heme proprionates themselves or the Lys86 residue, as its mutation to an alanine results in only a single conformer being favored at pH 8 (Figure 3A). Because of the structural flexibility and chemical nature of lysine, Lys86 plays a role in stabilizing two apparent conformations of NarI. In the wild-type/G65A enzyme, these two conformations correspond to quinone-bound (g = 3.33/3.52) and quinone-free (g = 3.18/3.23) NarI. Therefore, the binding of quinones and Q-site inhibitors to NarI modulates the electrochemical (E_m and pK_a) and g_z value of heme b_D in a Lys86-dependent manner. The exact role of Lys86 and quinol binding/oxidation is still a very active area of investigation in the field.

In conclusion, we have observed that the heterogeneity exhibited in EPR signals of heme b_D of *E. coli* nitrate reductase A is dependent upon growth conditions. Heterogeneity does not arise from effects of cardiolipin binding, but it most probably arises from differences in Q-site occupancy, where these differences can modulate heme b_D EPR signal position, reduction potential, and pH dependence of reduction potential. Our work indicates that careful analysis of redox titrations of NarGHI should be done in membranes prepared from cells grown very microaerobically and preferably in a cytochrome *bd* deletion strain.

■ ASSOCIATED CONTENT

Supporting Information

Results of the cytochrome *bd* and bo_3 deletions on NarGHI EPR heme spectra as well as anaerobic growth curves for NarGHI, NarGHI-K86A, NarGHI-G65A, and the background strain, LCB79. This material is available free of charge via the Internet at http://pubs.acs.org.

■ AUTHOR INFORMATION

Corresponding Author

*Phone (office): 780-492-2761; Phone (lab): 780-492-2558; Fax: 780-492-0886; E-mail: joel.weiner@ualberta.ca.

Present Address

†(K.S.G.) Department of Medicine, McMaster University, Hamilton, Ontario.

Funding

This work was funded by the Canadian Institutes of Health Research (FRN: 106550). Justin Fedor was supported by studentships from the Killam Trusts Foundation and Alberta Innovates: Health Solutions.

Notes

The authors declare no competing financial interest.

■ ACKNOWLEDGMENTS

We thank Francesca Sebastian and Nicholas Chua for their fantastic technical support.

■ ABBREVIATIONS USED

b_D, *b*-heme distal to NarGH; b_P, *b*-heme proximal to NarGH; CHES, *N*-cyclohexyl-2-aminoethanesulfonic acid; DDM, dodecylmaltoside; *E. coli*, *Escherichia coli*; E_h, applied potential; $E_{m,7}$, reduction potential at pH 7.0; EPR, electron paramagnetic resonance; FS4, [3Fe−4S]; GPF, glycerol-peptone-fumarate; HALS, highly anisotropic low spin; HOQNO, 2-*n*-heptyl 4-hydroxyquinoline-*N*-oxide; IPTG, isopropyl-1-thio-β-D-galactopyranoside; MES, 2-(*N*-morpholino)ethanesulfonic acid; MobisPGD, molybdo-bis(pyranopterin guanine dinucleotide); MOPS, 3-(*N*-morpholino)propanesulfonic acid; MQ, menaquinone; MWP, microwave power; NarGHI, *E. coli* nitrate reductase A; PB, plumbagin; PCP, pentachlorophenol; UQ, ubiquinone

■ REFERENCES

(1) Wimpenny, J. W. T., and Cole, J. A. (1967) The regulation of metabolism in facultative bacteria III. The effect of nitrate. *Biochim. Biophys. Acta, Gen. Subj. 148*, 233−242.

(2) Richardson, D. J., and Watmough, N. J. (1999) Inorganic nitrogen metabolism in bacteria. *Curr. Opin. Chem. Biol. 3*, 207−219.

(3) Blasco, F., Guigliarelli, B., Magalon, A., Asso, M., Giordano, G., and Rothery, R. A. (2001) The coordination and function of the redox centres of the membrane-bound nitrate reductases. *Cell. Mol. Life Sci. 58*, 179−193.

(4) Bertero, M. G., Rothery, R. A., Palak, M., Hou, C., Lim, D., Blasco, F., Weiner, J. H., and Strynadka, N. C. (2003) Insights into the respiratory electron transfer pathway from the structure of nitrate reductase A. *Nat. Struct. Biol. 10*, 681−687.

(5) Guigliarelli, B., Asso, M., More, C., Augier, V., Blasco, F., Pommier, J., Giordano, G., and Bertrand, P. (1992) EPR and redox characterization of iron-sulfur centers in nitrate reductases A and Z from *Escherichia coli*. Evidence for a high-potential and a low-potential class and their relevance in the electron-transfer mechanism. *Eur. J. Biochem. 207*, 61−68.

(6) Johnson, M. K., Bennett, D. E., Morningstar, J. E., Adams, M. W., and Mortenson, L. E. (1985) The iron-sulfur cluster composition of *Escherichia coli* nitrate reductase. *J. Biol. Chem. 260*, 5456−5463.
(7) Hackett, N. R., and Bragg, P. D. (1982) The association of two distinct *b* cytochromes with the respiratory nitrate reductase of *Escherichia coli*. *FEMS Microbiol. Lett. 13*, 213−217.
(8) Magalon, A., Rothery, R. A., Giordano, G., Blasco, F., and Weiner, J. H. (1997) Characterization by electron paramagnetic resonance of the role of the *Escherichia coli* nitrate reductase (NarGHI) iron-sulfur clusters in electron transfer to nitrate and identification of a semiquinone radical intermediate. *J. Bacteriol. 179*, 5037−5045.
(9) Rothery, R. A., Magalon, A., Giordano, G., Guigliarelli, B., Blasco, F., and Weiner, J. H. (1998) The molybdenum cofactor of *Escherichia coli* nitrate reductase A (NarGHI). Effect of a *mobAB* mutation and interactions with [Fe-S] clusters. *J. Biol. Chem. 273*, 7462−7469.
(10) Rothery, R. A., Blasco, F., Magalon, A., Asso, M., and Weiner, J. H. (1999) The hemes of *Escherichia coli* nitrate reductase A (NarGHI): Potentiometric effects of inhibitor binding to narI. *Biochemistry 38*, 12747−12757.
(11) Bertero, M. G., Rothery, R. A., Boroumand, N., Palak, M., Blasco, F., Ginet, N., Weiner, J. H., and Strynadka, N. C. (2005) Structural and biochemical characterization of a quinol binding site of *Escherichia coli* nitrate reductase A. *J. Biol. Chem. 280*, 14836−14843.
(12) Wallace, B. J., and Young, I. G. (1977) Role of quinones in electron transport to oxygen and nitrate in *Escherichia coli*. Studies with a *ubiA*$^-$ *menA*$^-$ double quinone mutant. *Biochim. Biophys. Acta, Bioenerg. 461*, 84−100.
(13) Lanciano, P., Vergnes, A., Grimaldi, S., Guigliarelli, B., and Magalon, A. (2007) Biogenesis of a respiratory complex is orchestrated by a single accessory protein. *J. Biol. Chem. 282*, 17468−17474.
(14) Arias-Cartin, R., Grimaldi, S., Pommier, J., Lanciano, P., Schaefer, C., Arnoux, P., Giordano, G., Guigliarelli, B., and Magalon, A. (2011) Cardiolipin-based respiratory complex activation in bacteria. *Proc. Natl. Acad. Sci. U.S.A. 108*, 7781−7786.
(15) Pascal, M. C., Burini, J. F., Ratouchniak, J., and Chippaux, M. (1982) Regulation of the nitrate reductase operon: Effect of mutations in *chlA*, *B*, *D* and *E* genes. *Mol. Gen. Genet. 188*, 103−106.
(16) Kikuchi, S., Shibuya, I., and Matsumoto, K. (2000) Viability of an *Escherichia coli pgsA* null mutant lacking detectable phosphatidylglycerol and cardiolipin. *J. Bacteriol. 182*, 371−376.
(17) Brondijk, T. H. C., Fiegen, D., Richardson, D. J., and Cole, J. A. (2002) Roles of NapF, NapG and NapH, subunits of the *Escherichia coli* periplasmic nitrate reductase, in ubiquinol oxidation. *Mol. Microbiol. 44*, 245−255.
(18) Baba, T., Ara, T., Hasegawa, M., Takai, Y., Okumura, Y., Baba, M., Datsenko, K. A., Tomita, M., Wanner, B. L., and Mori, H. (2006) Construction of *Escherichia coli* K-12 in-frame, single-gene knockout mutants: The Keio collection. *Mol. Syst. Biol. 2*, 2006.0008-1−2006.0008-11.
(19) Guigliarelli, B., Magalon, A., Asso, M., Bertrand, P., Frixon, C., Giordano, G., and Blasco, F. (1996) Complete coordination of the four Fe-S centers of the β subunit from *Escherichia coli* nitrate reductase. Physiological, biochemical, and EPR characterization of site-directed mutants lacking the highest or lowest potential [4Fe-4S] clusters. *Biochemistry 35*, 4828−4836.
(20) Sambrook, J., and Russell, D. W. (2001) *Molecular Cloning: A Laboratory Manual*, CSHL Press, Cold Spring Harbor, NY.
(21) Bilous, P. T., and Weiner, J. H. (1985) Dimethyl sulfoxide reductase activity by anaerobically grown *Escherichia coli* HB101. *J. Bacteriol. 162*, 1151−1155.
(22) Rothery, R. A., and Weiner, J. H. (1996) Interaction of an engineered [3Fe-4S] cluster with a menaquinol binding site of *Escherichia coli* DMSO reductase. *Biochemistry 35*, 3247−3257.
(23) Rothery, R. A., Blasco, F., and Weiner, J. H. (2001) Electron transfer from heme b_L to the [3Fe-4S] cluster of *Escherichia coli* nitrate reductase A (NarGHI). *Biochemistry 40*, 5260−5268.
(24) Weil, J. A. (2007) *Electron Paramagnetic Resonance: Elementary Theory and Practical Applications*, Wiley-Interscience, Hoboken, NJ.
(25) Bou-Abdallah, F., and Chasteen, N. D. (2008) Spin concentration measurements of high-spin ($g' = 4.3$) rhombic iron(III) ions in biological samples: Theory and application. *J. Biol. Inorg. Chem. 13*, 15−24.
(26) Markwell, M. A., Haas, S. M., Bieber, L. L., and Tolbert, N. E. (1978) A modification of the Lowry procedure to simplify protein determination in membrane and lipoprotein samples. *Anal. Biochem. 87*, 206−210.
(27) Lowry, O. H., Rosebrough, N. J., Farr, A. L., and Randall, R. J. (1951) Protein measurement with the Folin phenol reagent. *J. Biol. Chem. 193*, 265−275.
(28) Rothery, R. A., Chatterjee, I., Kiema, G., McDermott, M. T., and Weiner, J. H. (1998) Hydroxylated naphthoquinones as substrates for *Escherichia coli* anaerobic reductases. *Biochem. J. 332*, 35−41.
(29) Unden, G., and Bongaerts, J. (1997) Alternative respiratory pathways of *Escherichia coli*: Energetics and transcriptional regulation in response to electron acceptors. *Biochim. Biophys. Acta 1320*, 217−234.
(30) Ingledew, W. J., and Poole, R. K. (1984) The respiratory chains of *Escherichia coli*. *Microbiol. Rev. 48*, 222−271.
(31) Polglase, W. J., Pun, W. T., and Withaar, J. (1966) Lipoquinones of *Escherichia coli*. *Biochim. Biophys. Acta 118*, 425−426.
(32) Wissenbach, U., Ternes, D., and Unden, G. (1992) An *Escherichia coli* mutant containing only demethylmenaquinone, but no menaquinone: Effects on fumarate, dimethylsulfoxide, trimethylamine N-oxide and nitrate respiration. *Arch. Microbiol. 158*, 68−73.
(33) Wissenbach, U., Kröger, A., and Unden, G. (1990) The specific functions of menaquinone and demethylmenaquinone in anaerobic respiration with fumarate, dimethylsulfoxide, trimethylamine N-oxide and nitrate by *Escherichia coli*. *Arch. Microbiol. 154*, 60−66.
(34) Arias-Cartin, R., Lyubenova, S., Ceccaldi, P., Prisner, T., Magalon, A., Guigliarelli, B., and Grimaldi, S. (2010) HYSCORE evidence that endogenous mena- and ubisemiquinone bind at the same Q site ($Q_{(D)}$) of *Escherichia coli* nitrate reductase A. *J. Am. Chem. Soc. 132*, 5942−5943.
(35) Rothery, R. A., Blasco, F., Magalon, A., and Weiner, J. H. (2001) The diheme cytochrome *b* subunit (NarI) of *Escherichia coli* nitrate reductase A (NarGHI): Structure, function, and interaction with quinols. *J. Mol. Microbiol. Biotechnol. 3*, 273−283.
(36) Lanciano, P., Magalon, A., Bertrand, P., Guigliarelli, B., and Grimaldi, S. (2007) High-stability semiquinone intermediate in nitrate reductase A (NarGHI) from *Escherichia coli* is located in a quinol oxidation site close to heme b_D. *Biochemistry 46*, 5323−5329.
(37) Rothery, R. A., Bertero, M. G., Spreter, T., Bouromand, N., Strynadka, N. C. J., and Weiner, J. H. (2010) Protein crystallography reveals a role for the FS0 cluster of *Escherichia coli* nitrate reductase A (NarGHI) in enzyme maturation. *J. Biol. Chem. 285*, 8801−8807.
(38) Lacapère, J.-J., Pebay-Peyroula, E., Neumann, J.-M., and Etchebest, C. (2007) Determining membrane protein structures: Still a challenge! *Trends Biochem. Sci. 32*, 259−270.
(39) Kühlbrandt, W. (1988) Three-dimensional crystallization of membrane proteins. *Q. Rev. Biophys. 21*, 429−477.
(40) Vinothkumar, K. R., and Henderson, R. (2010) Structures of membrane proteins. *Q. Rev. Biophys. 43*, 65−158.
(41) Magalon, A., Rothery, R. A., Lemesle-Meunier, D., Frixon, C., Weiner, J. H., and Blasco, F. (1998) Inhibitor binding within the NarI subunit (cytochrome b_{nr}) of *Escherichia coli* nitrate reductase A. *J. Biol. Chem. 273*, 10851−10856.
(42) Unden, G. (1988) Differential roles for menaquinone and demethylmenaquinone in anaerobic electron transport of *E. coli* and their fnr-independent expression. *Arch. Microbiol. 150*, 499−503.
(43) Maklashina, E., and Cecchini, G. (2010) The quinone-binding and catalytic site of complex II. *Biochim. Biophys. Acta 1797*, 1877−1882.
(44) Walker, F. A., Huynh, B. H., Scheidt, W. R., and Osvath, S. R. (1986) Models of the cytochromes *b*. 6. The effect of axial ligand plane orientation on the EPR and Mössbauer spectra of low-spin ferrihemes. *J. Am. Chem. Soc. 108*, 5288−5297.

(45) Giordani, R., Buc, J., Cornish-Bowden, A., and Cárdenas, M. L. (1997) Kinetics of membrane-bound nitrate reductase A from *Escherichia coli* with analogues of physiological electron donors—different reaction sites for menadiol and duroquinol. *Eur. J. Biochem. 250*, 567−577.
(46) Kong, M. K., and Lee, P. C. (2011) Metabolic engineering of menaquinone-8 pathway of *Escherichia coli* as a microbial platform for vitamin K production. *Biotechnol. Bioeng. 108*, 1997−2002.
(47) Grimaldi, S., Arias-Cartin, R., Lanciano, P., Lyubenova, S., Szenes, R., Endeward, B., Prisner, T. F., Guigliarelli, B., and Magalon, A. (2012) Determination of the proton environment of high stability menasemiquinone intermediate in *Escherichia coli* nitrate reductase A by pulsed EPR. *J. Biol. Chem. 287*, 4662−4670.
(48) Grimaldi, S., Arias-Cartin, R., Lanciano, P., Lyubenova, S., Endeward, B., Prisner, T. F., Magalon, A., and Guigliarelli, B. (2010) Direct evidence for nitrogen ligation to the high stability semiquinone intermediate in *Escherichia coli* nitrate reductase A. *J. Biol. Chem. 285*, 179−187.
(49) Mikami, S., Tai, H., and Yamamoto, Y. (2009) Effect of the redox-dependent ionization state of the heme propionic acid side chain on the entropic contribution to the redox potential of *Pseudomonas aeruginosa* cytochrome c_{551}. *Biochemistry 48*, 8062−8069.
(50) Takayama, S. J., Mikami, S., Terui, N., Mita, H., Hasegawa, J., Sambongi, Y., and Yamamoto, Y. (2005) Control of the redox potential of *Pseudomonas aeruginosa* cytochrome c_{551} through the Fe−Met coordination bond strength and pK_a of a buried heme propionic acid side chain. *Biochemistry 44*, 5488−5494.
(51) Das, D. K., and Medhi, O. K. (1998) The role of heme propionate in controlling the redox potential of heme: Square wave voltammetry of protoporphyrinato IX iron(III) in aqueous surfactant micelles. *J. Inorg. Biochem. 70*, 83−90.
(52) DeLano, W. L. (2002) *The PyMOL Molecular Graphics System*, Schrödinger, LLC, New York.